Curing potential of experimental resin composites filled with bioactive glass: A comparison between Bis-EMA and UDMA based resin systems

Par, Matej ; Spanovic, Nika ; Mohn, Dirk ; Attin, Thomas ; Tauböck, Tobias T ; Tarle, Zrinka

Abstract: OBJECTIVES To evaluate the degree of conversion, light transmittance, and depth of cure of two experimental light-curable bioactive glass (BG)-containing composite series based on different resin systems. METHODS Experimental composite series based on either Bis-EMA or UDMA resin were prepared. Each series contained 0, 5, 10, 20, and 40wt% of BG 45S5. Reinforcing fillers were added up to a total filler load of 70wt%. The degree of conversion was evaluated using Raman spectroscopy, while light transmittance was measured using visible light spectroscopy. The depth of cure was estimated from the degree of conversion data and using the ISO 4049 scraping test. RESULTS Replacement of reinforcing fillers with BG can diminish the degree of conversion, light transmittance, and depth of cure. The effect of BG on the aforementioned properties was highly variable between the experimental series. While in the Bis-EMA series, the degree of conversion was significantly impaired by BG, all of the composites in the UDMA series attained clinically acceptable degree of conversion values. The reduction of the degree of conversion in the Bis-EMA series occurred independently of the changes in light transmittance. The UDMA series showed better light transmittance and consequently higher depth of cure than the Bis-EMA series. The depth of cure for all composites in the UDMA series was above 2mm. SIGNIFICANCE While the Bis-EMA series demonstrated clinically acceptable curing potential only for 0-10wt% of BG loading, an excellent curing potential in the UDMA series was observed for a wide range (0-40wt%) of BG loadings.

DOI: https://doi.org/10.1016/j.dental.2020.03.015

Curing potential of experimental resin composites filled with bioactive glass:

A comparison between Bis-EMA and UDMA based resin systems

Matej Par [a*], mpar@sfzg.hr,

Nika Spanovic [b], spanovic.nika5@gmail.com

Dirk Mohn [c,d], dirk.mohn@chem.ethz.ch

Thomas Attin [c], thomas.attin@zzm.uzh.ch

Tobias T. Tauböck [c], tobias.tauboeck@zzm.uzh.ch

Zrinka Tarle [a], tarle@sfzg.hr

[a] Department of Endodontics and Restorative Dentistry, School of Dental Medicine, University of Zagreb, Gunduliceva 5, Zagreb, Croatia

[b] Community Health Center, Zagreb, Croatia

[c] Department of Preventive Dentistry, Periodontology and Cariology, Center for Dental Medicine, University of Zurich, Plattenstrasse 11, CH-8032 Zurich, Switzerland

[d] Institute for Chemical and Bioengineering, Department of Chemistry and Applied Biosciences, ETH Zurich, Switzerland

* Corresponding author

Address for correspondence:

Matej Par
Department of Endodontics and Restorative Dentistry
School of Dental Medicine, University of Zagreb
Gunduliceva 5, Zagreb, Croatia
Tel. +385 91 739 3225
E-mail: mpar@sfzg.hr

Key words: bioactive glass 45S5, experimental composites, bioactive composites, degree of conversion, light transmittance, depth of cure

Abstract

Objectives. To evaluate the degree of conversion, light transmittance, and depth of cure of two experimental light-curable bioactive glass (BG)-containing composite series based on different resin systems.

Methods. Experimental composite series based on either Bis-EMA or UDMA resin were prepared. Each series contained 0, 5, 10, 20, and 40 wt% of BG 45S5. Reinforcing fillers were added up to a total filler load of 70 wt%. The degree of conversion was evaluated using Raman spectroscopy, while light transmittance was measured using visible light spectroscopy. The depth of cure was estimated from the degree of conversion data and using the ISO 4049 scraping test.

Results. Replacement of reinforcing fillers with BG can diminish the degree of conversion, light transmittance, and depth of cure. The effect of BG on the aforementioned properties was highly variable between the experimental series. While in the Bis-EMA series, the degree of conversion was significantly impaired by BG, all of the composites in the UDMA series attained clinically acceptable degree of conversion values. The reduction of the degree of conversion in the Bis-EMA series occurred independently of the changes in light transmittance. The UDMA series showed better light transmittance and consequently higher depth of cure than the Bis-EMA series. The depth of cure for all composites in the UDMA series was above 2 mm.

Significance. While the Bis-EMA series demonstrated clinically acceptable curing potential only for 0–10 wt% of BG loading, an excellent curing potential in the UDMA series was observed for a wide range (0–40 wt%) of BG loadings.

Key words: bioactive glass 45S5, experimental composites, bioactive composites, degree of conversion, light transmittance, depth of cure

1. Introduction

The addition of various functional fillers into resin composites has been investigated as a means to prevent secondary caries and increase restoration longevity [1]. Secondary caries has often been mentioned as the most common reason for composite restoration replacement, while about 60 % of all restorative procedures are related to the replacement of failed restorations, [2]. Among the various compounds which are being used for functionalizing experimental resin composites, bioactive glasses (BGs) are interesting candidates due to their potential to exert various beneficial effects when embedded into light-curable methacrylate resins, including remineralization of dental hard tissues [3], deposition of hydroxyapatite precipitates [4], inhibition of bacterial penetration through the microgap [5], antibacterial activity [6], and favorable biocompatibility [7]. Unlike enamel, in which an increased mineral content generally translates into improved mechanical properties, dentin is more challenging to remineralize because its mechanical properties are improved only if intrafibrillar mineralization is attained [8].

BGs encompass a heterogeneous group of substances of varying compositions, which determine their properties. The basic BG 45S5 composition (45 wt% SiO_2, 24.5 wt% CaO, 24.5 wt% Na_2O, and 6 wt% P_2O_5) is generally more reactive than compositions with lower sodium content [9]. Composites admixed with unsilanized BG 45S5 fillers have shown high solubility, which implies high bioactive potential [10]. This comes at the cost of mechanical properties [11], which tend to be better in composites containing more stable BG compositions [12].

An experimental light-curable composite series with a total filler load of 70 wt% and variable amounts of unsilanized BG 45S5 (0–40 wt%) in a Bis-GMA/TEGDMA resin matrix has recently been investigated on their curing potential [13] and polymerization kinetics [14]. These studies showed that the replacement of reinforcing fillers with BG can diminish curing efficiency, which was manifested as a decrease in the degree of conversion (DC) and depth of cure (DoC) [13], as well as reduced polymerization rate [14]. The negative effect of BG 45S5 on resin polymerization was observed independently of the changes in light transmittance and was ascribed to a premature termination of free-radical-mediated polymerization by the oxides on the surface of unsilanized BG fillers. The BG-induced polymerization inhibition can be partly responsible for impaired performance that was

reported for the aforementioned experimental series, including reduced flexural strength/modulus [11] and dentin bond strength [15], as well as increased water sorption and solubility [10].

Due to these drawbacks of Bis-GMA/TEGDMA resin [10,11,13–15], alternative resin systems were sought in order to achieve better polymerization of experimental BG-containing composites. This study aimed to investigate the curing potential of Bis-EMA/TEGDMA and UDMA/TEGDMA resin systems by evaluating the DC, light transmittance, and DoC in composite series containing 0–40 wt% of BG, using the same study design as that performed previously for the Bis-GMA/TEGDMA resin system [13]. The DC of experimental composites was evaluated in relation to the resin system, BG amount, layer thickness, and curing time. Light transmittance for 2-mm layers was assessed as a function of the resin system and BG amount. The DoC was estimated as the layer thickness at which the DC amounts to 80 % of the maximum attainable DC, and according to the ISO 4049 scraping test. The null hypotheses were that (I) the DC, (II) the light transmittance, and (III) the DoC of the experimental composite series would not differ between the two resin systems investigated.

2. Materials and methods

2.1 Resin composites

Two experimental composite series with varying amounts of BG (0–40 wt%) were prepared based on Bis-EMA/TEGDMA and UDMA/TEGDMA resin systems (Table 1). The BG fillers were used without surface silanization, whereas the reinforcing fillers (barium glass and silica) were silanized. The filler compositions followed a previous study on experimental composites based on a Bis-GMA/TEGDMA resin system [13]. The composite series were designated according to their base monomer and abbreviated as “Bis-EMA series” and “UDMA series”, respectively.

The weight ratios of base and diluent monomers were adjusted in order to incorporate 70 wt% of fillers, including nanometer-sized silica particles with a large surface area. Expressed in mole ratios, the percentage of the base monomers Bis-EMA and UDMA in the corresponding resin systems were 44.3 and 70.9 %, respectively. These ratios were within the usual range for commercial resin composites [16].

The resinous phase, photoinitiator, and co-initiator were mixed using a magnetic stirrer for 48 h. The obtained mixture was subsequently mixed with reinforcing fillers and BG using a dual asymmetric

centrifugal mixing system (Speed Mixer TM DAC 150 FVZ, Hauschild & Co. KG, Hamm, Germany) at 2700 rpm. The mixing was performed in five one-minute intervals separated by one-minute breaks to avoid overheating. After mixing, the obtained materials were deaerated in vacuum for 12 h.

As a reference material, a commercial composite with bioactive fillers (Beautifil II, shade: A2, LOT: 051829, Shofu, Kyoto, Japan) was used. That material is based on a Bis-GMA/TEGDMA resin system filled with 83 wt% (69 vol%) of fluoroboraluminosilicate glass, including surface pre-reacted glass fillers.

2.2 Degree of conversion

The DC as a function of layer thickness was measured using a previously developed setup for Raman spectroscopy [13]. Cylindrical specimens (d = 3 mm, h = 5 mm) were prepared by inserting composite pastes into custom-made stainless-steel split-molds, covering both mold apertures with a polyethylene terephthalate (PET) strip and light-curing through the upper mold aperture. A wide spectrum light-emitting diode (LED) curing unit was used (Bluephase G2, Ivoclar Vivadent, Schaan, Liechtenstein; wavelength range 380–515 nm, radiant exitance of 1185 mW/cm^2, as measured using integrating sphere, IS, Gigahertz-Optik GmbH, Puchheim, Germany and spectrometer HR4000, Ocean Optics, Dunedin, FL, USA). The curing unit tip was positioned perpendicularly above the upper mold aperture (0 mm from the composite surface) and the curing unit was activated for 20 and 40 s, resulting in total radiant exposures at the composite surface of 23.7 and 47.4 J/cm^2, respectively. The environmental temperature during light-curing was 21 ± 1 °C. Raman spectra were collected immediately after light-curing from the upper specimen surface, which was denoted as the thickness of 0 mm. The specimens were subsequently transferred to an incubator (Cultura, Ivoclar Vivadent) for a dark storage during 24 h at 37 ± 1 °C and 40 % ± 15 % relative humidity. After that post-cure period, Raman spectra were collected from five precisely determined points on composite specimens, representing layer thicknesses of 0, 1, 2, 3, and 4 mm.

Raman spectroscopy was performed using an FT-Raman spectrometer (Spectrum GX, PerkinElmer, Waltham, MA, USA) with an excitation NdYaG laser of 1064 nm wavelength, laser power of 800 mW, and spectral resolution of 4 cm^{-1}. The excitation laser was pointed at the most prominent part of the cylindrical specimen surface which was positioned in the collecting lens focus with an excited diameter of 0.3 mm. For each spectrum, 40 scans were recorded with an overall collection time of 8

min. The same parameters were used to collect Raman spectra of uncured composite pastes (n = 5). Raman spectra were processed with the Kinetics add-on for Matlab (version 7.5.0 MathWorks, Natick, MA, USA).

The DC was calculated through the relative change in the peak height of the spectral band at 1640 cm^{-1} (aliphatic C=C stretching), whereas the bands at 1610 cm^{-1} (aromatic C=C stretching) and 1458 cm^{-1} (C-H stretching) were used as reference bands for Bis-EMA and UDMA series, respectively. For Beautifil II, the band at 1610 cm^{-1} was used as a reference. The DC was calculated according to the following equation:

$$DC\ (\%) = \left(1 - \frac{(1640\ cm^{-1}\ /\ reference)_{peak\ height\ after\ curing}}{(1640\ cm^{-1}\ /\ reference\ )_{peak\ height\ before\ curing}}\right) x\ 100$$

A total of 100 specimens were prepared for all combinations of investigated factors (2 resin systems, 5 BG amounts, 2 curing times, and 5 experimental runs for each group) and 6 measurements were performed on each specimen (0 mm immediately after curing, and 0–4 mm after 24 h), resulting in a total of 600 DC values available for the analysis using a full-factorial ANOVA model.

For the DoC estimation, mean DC values were plotted against the composite layer thickness and the thickness corresponding to 80 % of the maximum attainable DC was recorded as the DoC [13].

2.3 Light transmittance

Light transmittance through 2-mm composite specimens was measured in real time during light-curing using Bluephase G2, as described previously [17]. Because light transmittance increased as the polymerization advanced, light-curing was performed for 60 s in order to capture the plateau, which signified that transmittance changes have stabilized. Composite specimens were prepared in black discoid Teflon molds (d = 6 mm, h = 2 mm) and sandwiched between two PET strips. The light that passed through composite specimens was collected by a lens and directed into a charge-coupled device array fiber spectrometer HR4000 (Ocean Optics, Dunedin, FL, USA), which recorded visible light spectra at a data collection rate of 20 s^{-1}. In the same manner, light spectra passing through the empty specimen compartment were recorded. Light transmittance (%) based on the integrated intensity of the whole curing unit emission spectrum (380–515 nm) was calculated as the following ratio:

$$Light\ transmittance\ (\%) = \frac{Light\ intensity\ (composite\ specimen)}{Light\ intensity\ (empty\ specimen\ compartment)}\ x\ 100$$

Light transmittance values for each time point during real-time measurements were plotted as a function of time. From these plots, light transmittance values from the start and the end of the curing period were recorded and denoted as “initial” and “final” light transmittance, respectively. Additionally, a parameter denoted as “effective transmittance” was calculated by integrating the light intensity curves for the whole 60-s period and dividing the obtained mathematical areas for composite specimen by the areas obtained for the empty specimen compartment. The effective transmittance calculated in this manner can be regarded as a single transmittance value which is representative for the whole curing period because it can be multiplied by the radiant exposure received at the specimen surface to calculate the radiant exposure which reached the specimen bottom [17]. Five experimental runs per group were performed. The environmental temperature during measurements was 21 ± 1 °C.

2.4 ISO 4049 depth of cure scraping test

The DoC according to ISO 4049 was evaluated for composite specimens (n = 5) light-cured under the identical conditions as described for the DC measurements (Bluephase G2, distance from the specimen of 0 mm, and exposure times of 20 and 40 s). Cylindrical specimens were prepared in stainless-steel split-molds (d = 4 mm, h = 14 mm) and the soft part of the composite was removed using a plastic spatula immediately after light-curing. Half-length of the remaining cylinder length was reported as the ISO 4049 DoC. The environmental temperature during measurements was 21 ± 1 °C.

2.5 Statistical analysis

Normality of distribution was assessed using Shapiro-Wilk’s test, while the uniformity of variances was evaluated using Levene’s test. The DC data were analyzed using a mixed model ANOVA with “thickness” as a within-subject factor and “resin system”, “BG amount”, and “curing time” as between-subject factors. The effect size of individual factors was assessed using partial eta-squared statistics. Pairwise comparisons of DC data between two curing times at fixed levels of other factors were performed using a t-test for independent observations. One-way ANOVA was used to analyze the light transmittance data for all combinations of different resin systems and BG amounts. The effect of the BG amount on ISO 4049 DoC was evaluated by comparing the DoC values among composites

with different BG amounts within each resin system and curing time using one-way ANOVA. For all ANOVA models, multiple comparisons were performed using Tukey and Bonferroni corrections for independent and dependent observations, respectively. As the DC and DoC data of experimental composites were analyzed using a full-factorial ANOVA, the statistical analysis for the DC and DoC of the commercial reference material was performed separately. Statistical analysis was performed in SPSS (version 20, IBM, Armonk, NY, USA) using an overall α value of 0.05.

3. Results

3.1 Degree of conversion

The results of the mixed model ANOVA presented in Table 2 indicate statistical significance (p values) and practical significance (partial η^2 values) of individual factors and their combinations. All of the factors had high statistical significance ($p<0.001$) and similar magnitudes of practical significance. Among the binary, ternary and quaternary interactions of individual factors, the largest effect size was identified for the interaction of the resin system and BG amount, as indicated by the corresponding partial η^2 of 0.966. Therefore, an additional mixed model ANOVA was performed for each resin system separately (Table 3). That analysis indicated that the BG amount had a more pronounced effect in the Bis-EMA series than in the UDMA series (partial η^2 of 0.991 and 0.898, respectively), whereas effect sizes of other individual factors were similar for both series. The DC data presented as a function of the BG amount, layer thickness, and curing time (Figures 1 and 2) also indicate that variations in the BG amount had a higher influence on the Bis-EMA series. In general, the DC was considerably more diminished by increasing the BG amount in the Bis-EMA series than in the UDMA-series. In the latter series, the post-cure DC values for BG amounts between 0–40 wt% were statistically similar for layer thicknesses of up to 1 mm (20 s curing time) or 2 mm (40 s curing time). In contrast, the post-cure DC values in the Bis-EMA series were statistically heterogeneous among different BG amounts for all layer thicknesses, even at the specimen surface (0 mm). At a clinically relevant layer thickness (up to 2 mm), doubling the curing time from 20 to 40 s resulted in a more pronounced improvement in the DC values in the Bis-EMA series, whereas comparatively smaller improvements were attained in the UDMA series.

Figure 3 shows the DC values for the commercial reference material. The post-cure DC values were statistically similar among layer thicknesses of 0–2 mm, regardless of the curing time. The DC

improvement due to the longer curing time (40 s) became more pronounced as the layer thickness increased.

3.2 Light transmittance

A representative plot of light intensity integrated across the full wavelength range (380–515 nm) is shown in Figure 4 to explain how “initial”, “final”, and “effective” light transmittance values were obtained. The plotted curves represent light intensity as a function of time for the composite specimen and for the empty specimen compartment. Dividing the former value by the latter at two particular time points (initial and final) gave the corresponding light transmittance values, whereas effective light transmittance was calculated as the ratio of the area below the curve of the composite specimen (red) and the area below the curve of the empty specimen compartment (blue).

Figure 5 shows initial and final light transmittance values (%) for the experimental series and commercial reference composite. In general, initial light transmittance of experimental composites filled with BG was lower than that of the commercial reference, but a considerable transmittance increase during curing of the experimental composites led to final transmittance values, which mostly surpassed light transmittance of the reference material. Figure 6 shows effective light transmittance, which summarizes transmittance variations throughout the whole curing period. For a given BG amount, composites in the Bis-EMA series showed lower effective light transmittance than the corresponding composites in the UDMA series. In both experimental series, the partial replacement of reinforcing fillers by BG resulted in a reduction of light transmittance. Nevertheless, an unexpectedly high light transmittance was observed for BG-20 in the UDMA series. Effective light transmittance of all composites in the UDMA series (with or without BG) was higher compared to the effective light transmittance of the reference material.

3.3 Depth of cure

The percentage of the maximum attainable DC is plotted as a function of layer thickness in Figure 7. For both experimental series and curing times, the DC decline through depths became steeper as the BG amount increased. The DC decline was more pronounced in the Bis-EMA series than in the UDMA series. The DoC was determined as the layer thickness which corresponds to the intersection of the DC curves with the dotted line denoting 80 % of the maximum attainable DC. The DoC values

determined in this manner are plotted as a function of the BG amount in Figure 8 a,b. The alternative approach based on ISO 4049 method provided different DoC values (Figure 8 c,d). Regardless of the differences in absolute DoC values, both approaches identified a negative relationship between the DoC and the BG amount for both experimental series. The UDMA series attained DoC values above or near 2 mm regardless of curing time or the DoC evaluation method (Figure 8 b,d), whereas the DoC of the Bis-EMA series dropped below 2 mm for BG amounts of 5–10 wt% (Figure 8 a,c).

Figure 9 shows the DC decline through depths and the DoC values for the commercial reference material. The DoC was above 2 mm for both DoC estimation methods and both curing times.

4. Discussion

This study evaluated the curing potential of two series of experimental composites (Bis-EMA and UDMA series), complementing a previous study that investigated the curing potential of an experimental Bis-GMA series [13]. Within each composite series, five resin composites containing various amounts of BG (0–40 wt%) were prepared and their curing potentials were evaluated through measurements of the DC, light transmittance, and DoC. Because all of these variables differed significantly between the resin systems, all three null hypotheses were rejected.

Previous studies on the Bis-GMA series have reported that unsilanized BG fillers caused a dose-dependent inhibition of polymerization, as evidenced by diminishing the maximum attainable DC, curing efficiency at depth, and polymerization rate [13,14]. In the present study, an even more pronounced inhibitory effect of BG was identified in the Bis-EMA series. A direct comparison of the results from the study on the Bis-GMA series [13] with those in the present study is possible due to identical methodologies. In the Bis-GMA series, composites containing BG amounts of 0, 5, 10, 20, and 40 wt% showed maximum attainable DC values (%, at specimen surface, 24 h post-cure) of 81.2, 79.6, 78.3, 72.1, and 62.5, respectively, while the composites in the Bis-EMA series evaluated under the same conditions reached maximum attainable DC values (%) of 88.3, 89.4, 68.7, 41.5, and 33.2. As expected, materials with low BG amounts (0–5 wt%) in the Bis-EMA series reached higher DC values than the corresponding materials in the Bis-GMA series due to comparatively better mobility of Bis-EMA [18]. However, for materials containing BG amounts of 10 wt% or more, the DC values in the Bis-EMA series were lower compared to the corresponding materials in the Bis-GMA series. It appears that the resin system of the Bis-EMA series was more sensitive to polymerization inhibition

by BG fillers than that of the Bis-GMA series, although the Bis-EMA resin system was more mobile and capable of reaching higher DC when filled only with reinforcing fillers. It should be noted that the above discussed maximum attainable DC values were measured on specimen surfaces. At that site, it is unlikely that the DC was diminished due to differences in light scattering [19]. It is therefore plausible that a direct inhibitory effect of BG on resin polymerization exists, which is not mediated by changes in light transmittance [13].

In contrast to the Bis-EMA series, the BG amount variations in the UDMA series had practically no effect on the DC values at clinically relevant layer thicknesses (0–2 mm). For these layer thicknesses, the maximum attainable DC values in the UDMA series ranged between 74.9 and 80.5 %, which was comparable to the DC measured for the commercial reference material (Figure 3), as well as to the DC of commercial composites reported in the literature [20]. In the UDMA series, BG-0, BG-5, and BG-20 reached clinically acceptable DC values of at least 55 % [21], even for 4-mm layers. This finding indicates the potential of the aforementioned materials for being used as bulk-fill materials. In this context, the issue of shrinkage stress should be addressed in future studies.

For the Bis-EMA series, initially low DC values measured for 20-s light-curing time at clinically relevant layer thicknesses (0–2 mm) were significantly increased by doubling the curing time. The DC improvement due to longer light-curing became more pronounced as the BG amount increased, indicating that the negative effect of BG on polymerization can be partly compensated by using higher radiant exposures. However, composites with the highest BG amounts (20 and 40 wt%) in the Bis-EMA series showed clinically unacceptable DC at 2 mm regardless of the curing time. In contrast, using the longer curing time in the UDMA series resulted in no DC improvement at 0 mm, suggesting that 20 s of curing was sufficient to reach the maximum attainable DC. An improvement in DC was observed at deeper composite layers when the curing time was extended to 40 s. However, this improvement was less extensive compared to that identified in the Bis-EMA series.

Overall, the curing potential of the UDMA series was superior to that of both the Bis-EMA series and the previously investigated Bis-GMA series [13], especially for composites with the highest BG amounts (20 and 40 wt%). The experimental composites in the UDMA series attained clinically acceptable DC values at 2 mm for all BG amounts investigated (0–40 wt%), whereas in the Bis-EMA series clinically acceptable DC values were reached only for materials containing up to 10 wt% of BG.

The literature data on polymerization inhibition caused by BG fillers in dental resin composites is scarce. Besides the previously discussed studies on a Bis-GMA series [13,14], some evidence for an inhibitory effect of BG has been reported for the addition of zinc-modified BG in a Bis-EMA/TEGDMA resin system [22] and for the addition of BG 45S5 in a Bis-GMA/TEGDMA resin system [23]. A BG-induced polymerization inhibition can be caused by the direct contact of methacrylate resin and oxides on unsilanized surfaces of BG fillers [24]. Such an explanation is supported by literature evidence on the inhibition of free-radical-mediated polymerization by electron-accepting oxides on the surface of filler particles, for example in epoxy [25], polyester [26], and methyl-methacrylate resins [27]. By the same mechanism, oxides on the surface of BG fillers could terminate the chain reaction in bifunctional methacrylate resins by inactivating growing macroradicals. A study using the same experimental composite series as the present study employed post-cure heating at 150 °C to distinguish whether the polymerization inhibition is caused by a direct (temperature-independent) effect of BG or an indirect (temperature-dependent) effect of restricted mobility of reactive species [28]. That study identified a limited potential of post-cure heating for improving DC, thereby providing evidence in favor of the direct mechanism of polymerization inhibition. In addition to the polymerization inhibition being dependent on the resin system, preliminary studies on fluoride-modified BG (data not shown) suggest that the BG composition can also affect its inhibitory potential.

In both experimental composite series, replacing the reinforcing fillers with BG reduced the total resin/filler interfacial surface area due to a comparatively larger particle size of BG fillers. The resulting reduction of composite viscosity was expected to improve the mobility of the resinous phase and allow the materials to reach higher DC [29]. However, this effect was not observed in either resin system, which can be ascribed to two main reasons. First, it is possible that an inhibitory effect of BG on polymerization counteracted the benefit gained from improved monomer mobility [13]. Second, silica nanoparticles tend to agglomerate due to their high surface area [30] and the size of agglomerates may have differed among composites with various BG amounts [31]. The size of silica agglomerates was difficult to control during the preparation of experimental composites because the size of secondary silica particles was affected by composition-dependent shear forces that occurred during mixing. There may be other possible explanations for the reduction of the interfacial surface area having no effect on the DC, but these were beyond the scope of the present study.

It is generally accepted that the maximum attainable DC of resin composites is diminished by higher loadings of silanized fillers due to increased viscosity caused by higher interfacial surface area [29]. The effect of unsilanized fillers in experimental composites appears less consistent, as these can either enhance or diminish the maximum DC, depending on their particle size and chemical composition. For example, replacing the silanized glass fillers with unsilanized amorphous calcium phosphate improved the final DC [32], whereas unsilanized BG [13] and silver nanoparticles [33] can reduce the final DC. As polymerization inhibition caused by BG fillers depends on their direct contact with the resinous matrix, it could theoretically be reversed by coating filler particles with a surface layer of silane [25,26]. That modification may be beneficial beyond possible DC improvements, as it can enhance mechanical properties by enabling chemical bonding between filler particles and the matrix [34]. However, surface silanization of bioactive particles reduces ion release [35], which is the rationale for the common use of unsilanized particles in remineralizing composites.

Light transmittance through 2-mm specimens of experimental composites increased during curing as a result of photoinitiator consumption and diminished light scattering [36,37]. The latter phenomenon commonly occurs in light-curable resin composites because the difference in refractive indices between the resinous matrix and fillers decreases as the polymerization progresses [38]. To evaluate the changes in light transmittance that occurred during curing, initial and final transmittance values were calculated from real-time light intensity curves (Figure 4). Initial light transmittance for all BG-containing experimental composites was significantly lower than that of the commercial reference material (Figure 5). However, the experimental composites showed a more extensive increase in light transmittance during curing (1.4–5.0 %) than the commercial reference composite (0.4 %). In this way, experimental composites were able to compensate for the disadvantage of initially lower light transmittance.

The initial and final light transmittance values provide limited information about the curing potential because these were obtained at two fixed time points, disregarding all the changes that occurred in between. To better describe curing light transmission throughout the whole curing period, effective light transmittance values were calculated (Figure 6). Within each experimental series, effective light transmittance declined with increasing BG amounts, except for BG-20 in the UDMA series, which showed an unexpectedly high value. The tendency of light transmittance to decline as reinforcing

fillers are being replaced with BG can be explained in terms of light scattering. The intensity of light scattering in resin composites is a function of filler particle size and the difference in refractive indices between fillers and the resin. The refractive indices of the components of experimental composites were as follows: Bis-EMA: 1.54, UDMA: 1.48, TEGDMA: 1.46, silica: 1.46, barium glass: 1.53, and BG: 1.56. Although the exact contribution of each of the distinct filler types to light scattering and the resulting light attenuation could not be determined, it is notable that BG had a higher refractive index than the reinforcing fillers. The decline in light transmittance as a result of increasing BG amounts in the Bis-EMA series can be explained in terms of the refractive index mismatch between BG fillers and the resin system. Although refractive indices of the base resin (Bis-EMA) and BG fillers were similar, the mole ratio of Bis-EMA was only 44.3%, whereas the remaining 55.7 % pertains to the diluent resin TEGDMA. Considering mole ratios, TEGDMA was the major constituent of the resin system, suggesting that the mismatch of its refractive index with that of BG may have caused the decline in light transmittance with the increasing amount of BG. In a similar manner, the declining pattern of light transmittance with higher BG amounts in the UDMA series can be explained by the replacement of reinforcing fillers, having refractive indices closer to those of UDMA and TEGDMA, with BG fillers which introduced a higher refractive index mismatch. An exception to the pattern of the reduction in light transmittance with higher BG amounts was identified only for BG-20 in UDMA series. It is difficult to speculate about the cause for that unexpected high light transmittance value, but it should be noted that the previous study on the Bis-GMA series also showed that light transmittance was not linearly related with the BG amount [13]. The non-linear relationship can be attributed to complex interactions of different particle size distributions, as well as to the difficulties in controlling the particle size of experimental composites. The inability to control the size of silica agglomerates that has been discussed before may also influence light scattering in experimental composites. As the agglomerate size approached half the wavelength of the curing light, amounting to approximately 0.2 μm, the light scattering intensified and consequently diminished light transmittance [39]. Because barium glass and BG particles were two orders of magnitude larger than silica nanoparticles, these fillers were less prone to agglomeration. Therefore, barium glass and BG were likely to exert a more consistent effect on light scattering.

The plots of the DC decline as a function of layer thickness in Figure 7 show how light transmittance of the experimental composite series affected their curing potential. The curves of DC decline were

generally steeper in the Bis-EMA series compared to the UDMA series, which can be attributed to the comparatively lower light transmittance of the Bis-EMA series. Within each experimental series and curing time, the curves became steeper as the BG amount was increased, reflecting the corresponding decline in light transmittance (Figure 6).

The DoC was estimated in two alternative ways: (I) as the layer thickness that corresponds to 80 % of the maximum attainable DC, and (II) as the half-length of the cylinder that remains after removal of the uncured material, according to the ISO 4049 scraping test. Because the addition of BG reduced light transmittance (Figure 6) and the DC at thicker layers (Figure 7), it was of particular interest to investigate the relationship between BG amount and DoC.

The DoC as a function of BG amount is shown in Figure 8. The UDMA series maintained the DoC above 2 mm for all BG amounts, whereas the DoC values in the Bis-EMA series decreased below 2 mm for BG amounts as low as 5–10 wt%. Additionally, all of the composites in the UDMA series showed higher DoC values than the corresponding composites in the Bis-EMA series. Doubling the curing time resulted in a modest DoC improvement in the Bis-EMA series, however, the DoC values in composites containing at least 10 wt% of BG remained well below 2 mm. In contrast, UDMA series showed a better response to the doubled curing time, as already high DoC values were further increased for 1.0–1.5 mm. The DoC in the UDMA series was also higher than that of the previously investigated Bis-GMA series [13], for which DoC dropped below 2 mm for BG amounts of 20–40 wt%. The favorable DoC of the UDMA series can be regarded as the result of better light transmittance (Figure 6) and insensitivity to polymerization inhibition by BG fillers (Figure 2).

For the commercial reference material, the DoC values were in accordance with the manufacturer's instructions for clinical use, namely 2.6–2.7 mm for 20 s curing time (Figure 9). The DoC values of the reference material were comparable to those in the UDMA series, both for the "80% of the maximum DC" and ISO 4049 method. In contrast, the DoC values in the Bis-EMA series were inferior to those of the reference material.

Considering the results of the present study together with the previously published data of a Bis-GMA series [13], the curing potential of the experimental composite series can be ranked as follows: UDMA series > Bis-GMA series > Bis-EMA series. These inferences are based on the resin systems in which the ratios of base and diluent monomers were chosen to attain viscosities suitable for the

incorporation of 70 wt% of fillers. Thus, no generalizations about the curing potential can be made for different ratios of base and diluent monomers. Because the relative amounts of base and diluent monomers determine the maximum attainable DC and mechanical properties [40], the fine-tuning of resin compositions remains a topic for future studies.

5. Conclusions

With regards to the degree of conversion, light transmittance, and depth of cure, the UDMA series of bioactive glass-modified composites demonstrated markedly better curing potential than the Bis-EMA series. Unlike the Bis-EMA series, the UDMA series showed no evidence of direct polymerization inhibition by the addition of bioactive glass 45S5 in mass fractions of 0–40 wt%. The higher light transmittance in the UDMA series was reflected in superior DoC values exceeding the 2-mm threshold for all investigated bioactive glass amounts. Due to its favorable curing potential, the UDMA series of experimental composites is a prospective candidate for subsequent investigations of bioactivity and mechanical properties.

Acknowledgments

The authors would like to thank Ozren Gamulin from the School of Medicine, University of Zagreb, Croatia for assistance with Raman spectrometry. Hrvoje Skenderovic from the Institute of Physics, Zagreb, Croatia is acknowledged for help with visible light spectrometry.

Declarations of interest: None

References

[1] Khan AS, Syed MR. A review of bioceramics-based dental restorative materials. Dent Mater J 2019;38:163–76.

[2] Eltahlah D, Lynch CD, Chadwick BL, Blum IR, Wilson NHF. An update on the reasons for placement and replacement of direct restorations. J Dent 2018;72:1–7.

[3] Tezvergil-Mutluay A, Seseogullari-Dirihan R, Feitosa VP, Cama G, Brauer DS, Sauro S. Effects of composites containing bioactive glasses on demineralized dentin. J Dent Res 2017;96:999–1005.

[4] Tauböck TT, Zehnder M, Schweizer T, Stark WJ, Attin T, Mohn D. Functionalizing a dentin bonding resin to become bioactive. Dent Mater 2014;30:868–75.

[5] Khvostenko D, Hilton TJ, Ferracane JL, Mitchell JC, Kruzic JJ. Bioactive glass fillers reduce bacterial penetration into marginal gaps for composite restorations. Dent Mater 2016;32:73–81.

[6] Chatzistavrou X, Velamakanni S, DiRenzo K, Lefkelidou A, Fenno JC, Kasuga T, et al. Designing dental composites with bioactive and bactericidal properties. Mater Sci Eng C 2015;52:267–72.

[7] Salehi S, Gwinner F, Mitchell JC, Pfeifer C, Ferracane JL. Cytotoxicity of resin composites containing bioactive glass fillers. Dent Mater 2015;31:195–203.

[8] Fernando D, Attik N, Pradelle-Plasse N, Jackson P, Grosgogeat B, Colon P. Bioactive glass for dentin remineralization: A systematic review. Mater Sci Eng C 2017;76:1369–77.

[9] Jones JR. Review of bioactive glass: From Hench to hybrids. Acta Biomater 2013;9:4457–86.

[10] Par M, Spanovic N, Bjelovucic R, Marovic D, Schmalz G, Gamulin O, et al. Long-term water sorption and solubility of experimental bioactive composites based on amorphous calcium phosphate and bioactive glass. Dent Mater J 2019;38: 555-64.

[11] Par M, Tarle Z, Hickel R, Ilie N. Mechanical properties of experimental composites containing bioactive glass after artificial aging in water and ethanol. Clin Oral Investig 2019;23:2733–41.

[12] Khvostenko D, Mitchell JC, Hilton TJ, Ferracane JL, Kruzic JJ. Mechanical performance of novel bioactive glass containing dental restorative composites. Dent Mater 2013;29:1139–48.

[13] Par M, Spanovic N, Bjelovucic R, Skenderovic H, Gamulin O, Tarle Z. Curing potential of experimental resin composites with systematically varying amount of bioactive glass: Degree of conversion, light transmittance and depth of cure. J Dent 2018;75:113–20.

[14] Par M, Tarle Z, Hickel R, Ilie N. Polymerization kinetics of experimental bioactive composites containing bioactive glass. J Dent 2018;76:83–8.

[15] Par M, Tarle Z, Hickel R, Ilie N. Dentin bond strength of experimental composites containing bioactive glass: changes during aging for up to 1 year. J Adhes Dent 2018;20:325–34.

[16] Barszczewska-Rybarek IM. Structure–property relationships in dimethacrylate networks based on Bis-GMA, UDMA and TEGDMA. Dent Mater 2009;25:1082–9.

[17] Par M, Repusic I, Skenderovic H, Tarle Z. Wavelength-dependent light transmittance in resin composites: practical implications for curing units with different emission spectra. Clin Oral Investig 2019;12:4399-409.

[18] Cornelio RB, Wikant A, Mjøsund H, Kopperud HM, Haasum J, Gedde UW, et al. The influence of bis-EMA vs bis GMA on the degree of conversion and water susceptibility of experimental composite materials. Acta Odontol Scand 2014;72:440–7.

[19] Leprince JG, Palin WM, Hadis MA, Devaux J, Leloup G. Progress in dimethacrylate-based dental composite technology and curing efficiency. Dent Mater 2013;29:139–56.

[20] Tarle Z, Par M. Degree of Conversion. In: Miletic V, editor. Dent. Compos. Mater. Direct Restor., Cham: Springer International Publishing; 2018, p. 63–85.

[21] Silikas N, Eliades G, Watts DC. Light intensity effects on resin-composite degree of conversion and shrinkage strain. Dent Mater 2000;16:292–6.

[22] Sfalcin RA, Correr AB, Morbidelli LR, Araújo TGF, Feitosa VP, Correr-Sobrinho L, et al. Influence of bioactive particles on the chemical-mechanical properties of experimental enamel resin infiltrants. Clin Oral Investig 2017;21:2143–51.

[23] Nicolae LC, Shelton RM, Cooper PR, Martin RA, Palin WM. The effect of UDMA/TEGDMA mixtures and bioglass incorporation on the mechanical and physical properties of resin and resin-based composite materials. Conf Pap Sci 2014;2014:1–5.

[24] Plueddemann EP. Silane Coupling Agents. New York: Springer-Verlag; 2013.

[25] Plueddemann EP. Catalytic effects in bonding thermosetting resins to silane-treated fillers. In: Deanin RD, Schott NR, editors. Fill. Reinf. Plast., vol. 134, Washington, D. C.: American Chemical Society; 1974, p. 86–94.

[26] Sen S, Nugay B. Tuning of final performances of unsaturated polyester composites with inorganic microsphere/platelet hybrid reinforcers. Eur Polym J 2001;37:2047–53.

[27] Solomon DH, Swift JD. Reactions catalyzed by minerals. Part II. Chain termination in free-radical polymerizations. J Appl Polym Sci 1967;11:2567–75.

[28] Par M, Spanovic N, Tauböck TT, Attin T, Tarle Z. Degree of conversion of experimental resin composites containing bioactive glass 45S5: the effect of post-cure heating. Sci Rep 2019;9:17245.

[29] Halvorson RH, Erickson RL, Davidson CL. The effect of filler and silane content on conversion of resin-based composite. Dent Mater 2003;19:327–33.

[30] Rahman IA, Padavettan V. Synthesis of silica nanoparticles by sol-gel: size-dependent properties, surface modification, and applications in silica-polymer nanocomposites—A review. J Nanomater 2012;2012:1–15.

[31] Antonucci JM, Skrtic D. Fine-tuning of polymeric resins and their interfaces with amorphous calcium phosphate. a strategy for designing effective remineralizing dental composites. Polymers 2010;2:378–92.

[32] Par M, Gamulin O, Marovic D, Skenderovic H, Klaric E, Tarle Z. Conversion and temperature rise of remineralizing composites reinforced with inert fillers. J Dent 2016;48:26–33.

[33] Barszczewska-Rybarek I, Chladek G. Studies on the curing efficiency and mechanical properties of bis-GMA and TEGDMA nanocomposites containing silver nanoparticles. Int J Mol Sci 2018;19:3937.

[34] Antonucci JM, Dickens SH, Fowler BO, Xu HHK; Chemistry of silanes: Interfaces in dental polymers and composites. J Res Natl Inst Stand Technol 2005;110:541.

[35] Braga RR. Calcium phosphates as ion-releasing fillers in restorative resin-based materials. Dent Mater 2019;35:3–14.

[36] Asmusen S, Arenas G, Cook WD, Vallo C. Photobleaching of camphorquinone during polymerization of dimethacrylate-based resins. Dent Mater 2009;25:1603–11.

[37] Emami N, Sjödahl M, Söderholm K-JM. How filler properties, filler fraction, sample thickness and light source affect light attenuation in particulate filled resin composites. Dent Mater 2005;21:721–30.

[38] Ilie N, Durner J. Polymerization kinetic calculations in dental composites: a method comparison analysis. Clin Oral Investig 2014;18:1587–96.

[39] Clewell DH. Scattering of Light by Pigment Particles. J Opt Soc Am 1941;31:521.

[40] Gonçalves F, Kawano Y, Pfeifer C, Stansbury JW, Braga RR. Influence of BisGMA, TEGDMA, and BisEMA contents on viscosity, conversion, and flexural strength of experimental resins and composites. Eur J Oral Sci 2009;117:442–6.

Table 1. Composition of experimental resin composites.

Material series	Material designation	Filler composition (wt%)		Total filler ratio (wt%)	Resin		Filler load (vol%)
		Bioactive glass	Reinforcing fillers (Ba:Si = 2:1)		wt%	Composition (wt%)	
Bis-EMA series	**BG-0**	0	70	70	30	60% Bis-EMA 40% TEGDMA photoinitiator system: 0.2% CQ 0.8% 4E	47
	BG-5	5	65	70	30		47
	BG-10	10	60	70	30		47
	BG-20	20	50	70	30		50
	BG-40	40	30	70	30		51
UDMA series	**BG-0**	0	70	70	30	80% UDMA 20% TEGDMA photoinitiator system: 0.2% CQ 0.8% 4E	47
	BG-5	5	65	70	30		47
	BG-10	10	60	70	30		47
	BG-20	20	50	70	30		50
	BG-40	40	30	70	30		51

Bioactive glass: SiO_2 45 wt%, Na_2O 24.5 wt%, CaO 24.5 wt%, P_2O_5 6 wt%, particle size (d50/d99 [µm]): 4.0/13.0, silanization: none, product name/manufacturer: G018-144/Schott, Mainz, Germany.

Barium-fillers (Ba): SiO_2 55.0 wt%, BaO 25.0 wt%, B_2O_3 10.0 wt%, Al_2O_3 10.0 wt%, particle size (d50/d99 [µm]): 1.0/4.0, silanization 3.2 wt%, product name/manufacturer: GM27884/Schott.

Silica-fillers (Si): $SiO_2 \geq 99.8$ wt%, primary particle size: 12 nm, silanization 4-6 wt%, product name/manufacturer: Aerosil DT/Evonik Degussa, Germany.

Bis-EMA: ethoxylated bisphenol A dimethacrylate, Esstech, PA, USA; TEGDMA: tri-ethylene glycol dimethacrylate, Esstech; UDMA: urethane dimethacrylate, Esstech; CQ: camphorquinone, Merck, Darmstadt; Germany; 4E: ethyl-4- (dimethylamino) benzoate, Merck.

Table 2. Results of the mixed model ANOVA indicating influences of individual factors and their interactions on the degree of conversion of experimental composites.

factor	p	partial η^2
resin system	<0.001	0.972
BG amount	<0.001	0.981
curing time	<0.001	0.926
thickness	<0.001	0.969
resin system * BG amount	<0.001	0.966
resin system * curing time	<0.001	0.358
resin system * thickness	<0.001	0.708
BG amount * curing time	0.008	0.156
BG amount * thickness	<0.001	0.657
curing time * thickness	<0.001	0.375
resin system * BG amount * curing time	<0.001	0.223
resin system * BG amount * thickness	<0.001	0.692
resin system * curing time * thickness	<0.001	0.394
BG amount * curing time * thickness	<0.001	0.381
resin system * BG amount * curing time * thickness	<0.001	0.430

Table 3. Results of the mixed model ANOVA for the degree of conversion data, performed separately for each resin system.

	Bis-EMA series		UDMA series	
Factor	p	partial η^2	p	partial η^2
BG amount	<0.001	0.991	<0.001	0.898
Curing time	<0.001	0.929	<0.001	0.926
Thickness	<0.001	0.968	<0.001	0.978
BG amount * curing time	0.029	0.232	<0.001	0.467
BG amount * thickness	<0.001	0.779	<0.001	0.863
Curing time * thickness	<0.001	0.148	<0.001	0.827

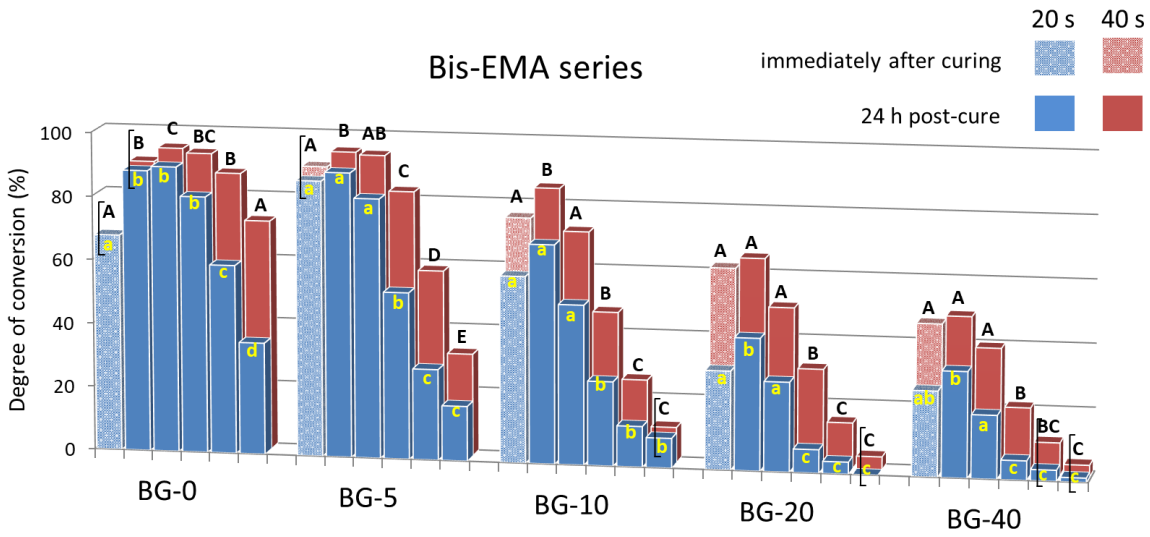

		20 s					40 s				
	Thickness	**BG-0**	**BG-5**	**BG-10**	**BG-20**	**BG-40**	**BG-0**	**BG-5**	**BG-10**	**BG-20**	**BG-40**
Immediately after curing	**0 mm**	67.8 (3.7)	86.6 (2.5)	58.5 (4.8)	31.0 (4.4)	26.9 (4.0)	66.3 (2.2)	89.6 (2.1)	75.3 (1.2)	61.5 (3.2)	46.1 (8.1)
24 h post- cure	**0 mm**	88.3 (1.9)	89.4 (2.2)	68.7 (6.1)	41.5 (3.4)	33.2 (4.0)	89.8 (0.9)	94.4 (1.6)	84.9 (0.6)	64.8 (5.1)	48.7 (4.0)
	1 mm	89.7 (2.4)	81.5 (1.5)	50.2 (7.5)	28.1 (2.8)	19.9 (3.4)	94.2 (1.0)	93.6 (2.1)	71.5 (2.5)	49.7 (3.9)	39.1 (3.1)
	2 mm	80.6 (2.6)	52.3 (6.9)	26.5 (5.1)	7.3 (3.6)	6.1 (2.4)	92.8 (0.7)	82.5 (1.6)	46.6 (5.0)	30.8 (3.8)	20.8 (1.3)
	3 mm	59.3 (8.0)	28.5 (5.3)	12.7 (3.7)	3.8 (7.7)	3.5 (4.4)	86.8 (0.8)	57.9 (5.1)	25.6 (6.2)	14.3 (1.4)	10.2 (5.2)
	4 mm	35.1 (10.3)	17.2 (3.7)	9.3 (7.7)	1.0 (8.1)	1.3 (4.6)	72.0 (3.7)	32.0 (5.3)	11.0 (5.2)	3.9 (7.0)	3.5 (4.1)

Figure 1. Mean values of the degree of conversion (%) as a function of BG amount, layer thickness, and curing time for Bis-EMA experimental series. Within each material, the leftmost bar denotes immediate conversion at the specimen surface (0 mm), while the subsequent bars from left to right denote 24 h post-cure conversion at depths of 0, 1, 2, 3, and 4 mm. Same letters above the bars denote statistically similar groups within a material and curing time (lowercase letters for 20 s and uppercase letters for 40 s). Square brackets connecting blue and red bars denote no difference between two curing times. Square brackets in the data table indicate statistically similar groups of values. Straight lines in the data table indicate statistically similar pairs of values. Standard deviations are given in parentheses.

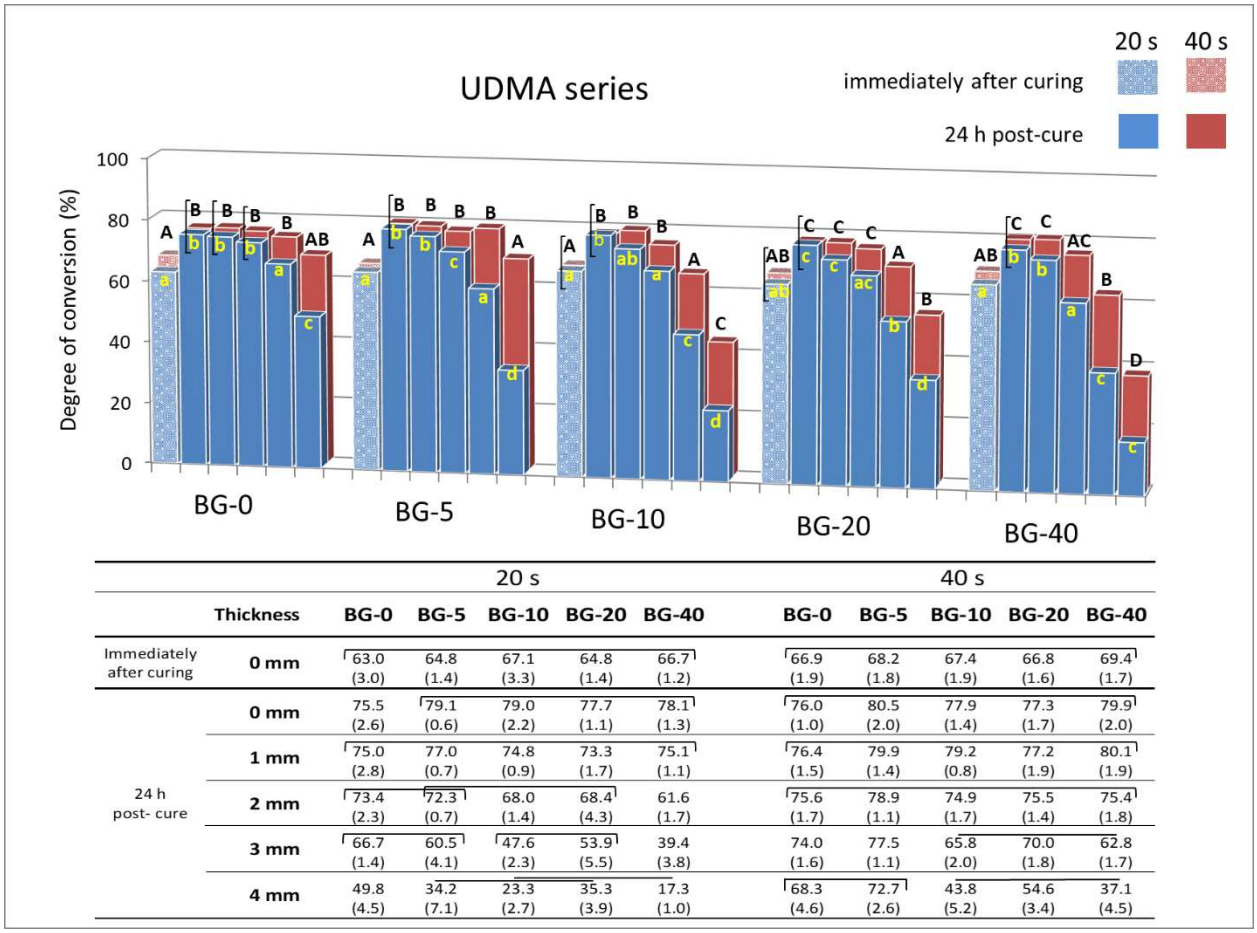

		20 s					40 s				
	Thickness	**BG-0**	**BG-5**	**BG-10**	**BG-20**	**BG-40**	**BG-0**	**BG-5**	**BG-10**	**BG-20**	**BG-40**
Immediately after curing	**0 mm**	63.0 (3.0)	64.8 (1.4)	67.1 (3.3)	64.8 (1.4)	66.7 (1.2)	66.9 (1.9)	68.2 (1.8)	67.4 (1.9)	66.8 (1.6)	69.4 (1.7)
24 h post- cure	**0 mm**	75.5 (2.6)	79.1 (0.6)	79.0 (2.2)	77.7 (1.1)	78.1 (1.3)	76.0 (1.0)	80.5 (2.0)	77.9 (1.4)	77.3 (1.7)	79.9 (2.0)
	1 mm	75.0 (2.8)	77.0 (0.7)	74.8 (0.9)	73.3 (1.7)	75.1 (1.1)	76.4 (1.5)	79.9 (1.4)	79.2 (0.8)	77.2 (1.9)	80.1 (1.9)
	2 mm	73.4 (2.3)	72.3 (0.7)	68.0 (1.4)	68.4 (4.3)	61.6 (1.7)	75.6 (1.7)	78.9 (1.1)	74.9 (1.7)	75.5 (1.4)	75.4 (1.8)
	3 mm	66.7 (1.4)	60.5 (4.1)	47.6 (2.3)	53.9 (5.5)	39.4 (3.8)	74.0 (1.6)	77.5 (1.1)	65.8 (2.0)	70.0 (1.8)	62.8 (1.7)
	4 mm	49.8 (4.5)	34.2 (7.1)	23.3 (2.7)	35.3 (3.9)	17.3 (1.0)	68.3 (4.6)	72.7 (2.6)	43.8 (5.2)	54.6 (3.4)	37.1 (4.5)

Figure 2. Mean values of the degree of conversion (%) as a function of BG amount, layer thickness, and curing time for UDMA experimental series. Within each material, the leftmost bar denotes immediate conversion at the specimen surface (0 mm), while the subsequent bars from left to right denote 24 h post-cure conversion at depths of 0, 1, 2, 3, and 4 mm. Same letters above the bars denote statistically similar groups within a material and curing time (lowercase letters for 20 s and uppercase letters for 40 s). Square brackets connecting blue and red bars denote no difference between two curing times. Square brackets in the data table indicate statistically similar groups of values. Straight lines in the data table indicate statistically similar pairs of values. Standard deviations are given in parentheses.

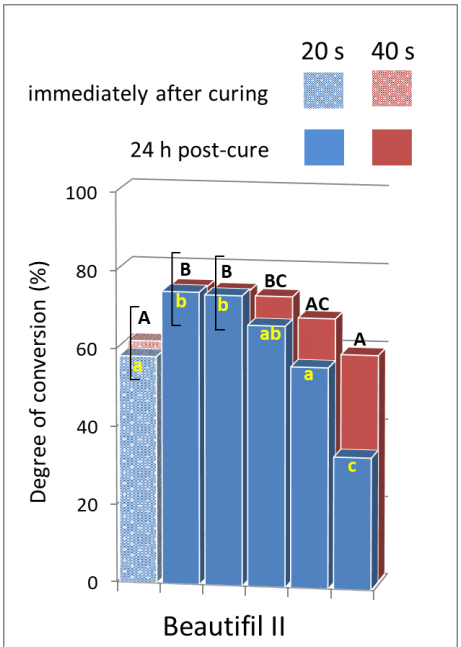

		20 s	40 s
Immediately after curing	0 mm	58.2 (0.9)	60.3 (4.3)
24 h post- cure	0 mm	74.9 (3.5)	74.6 (2.5)
	1 mm	74.3 (3.4)	73.9 (1.6)
	2 mm	66.9 (5.2)	72.6 (3.0)
	3 mm	56.6 (5.1)	67.3 (2.9)
	4 mm	33.9 (7.3)	58.2 (1.1)

Figure 3. Mean values of the degree of conversion (%) as a function of layer thickness and curing time for the commercial reference material. The leftmost bar denotes immediate conversion at the specimen surface (0 mm), while the subsequent bars from left to right denote 24 h post-cure conversion at depths of 0, 1, 2, 3, and 4 mm. Same letters above the bars denote statistically similar groups within a curing time (lowercase letters for 20 s and uppercase letters for 40 s). Square brackets connecting blue and red bars denote no difference between two curing times. Standard deviations are given in parentheses.

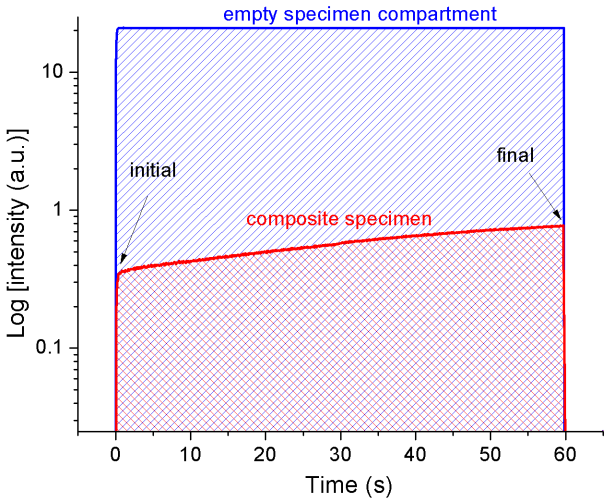

Figure 4. An example of real-time light intensity curves used to calculate “initial”, “final”, and “effective” values of light transmittance (material BG-20 in Bis-EMA series). Logarithmic scale is used for y-axis in order to better represent light intensities which differed by 1.5 orders of magnitude.

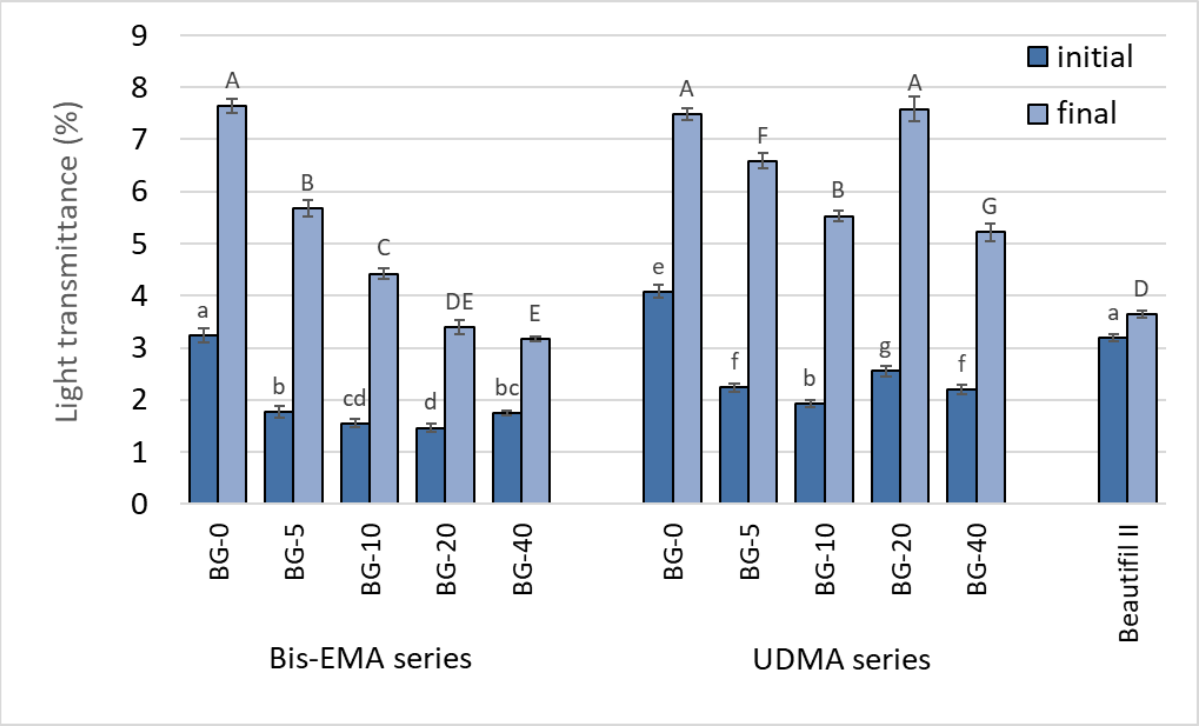

Figure 5. Mean values of light transmittance (%) recorded at the start (initial) and at the end (final) of the light-curing period. Within each material, the difference between initial and final transmittance values was statistically significant ($p<0.001$). Statistically similar groups within initial and final values are indicated by same lowercase and uppercase letters, respectively. Error bars indicate ± 1 s.d.

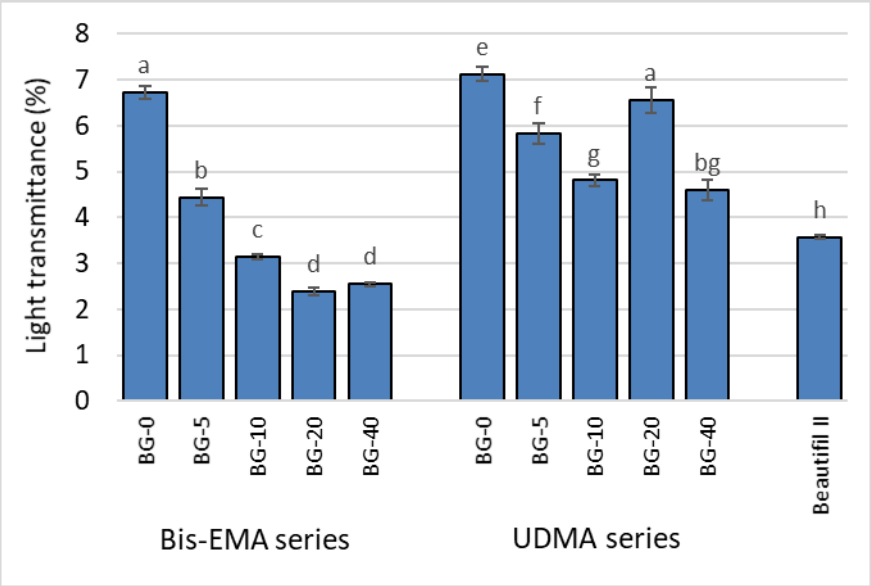

Figure 6. Mean values of effective light transmittance (%). Statistically similar groups are indicated by same lowercase letters. Error bars indicate ± 1 s.d.

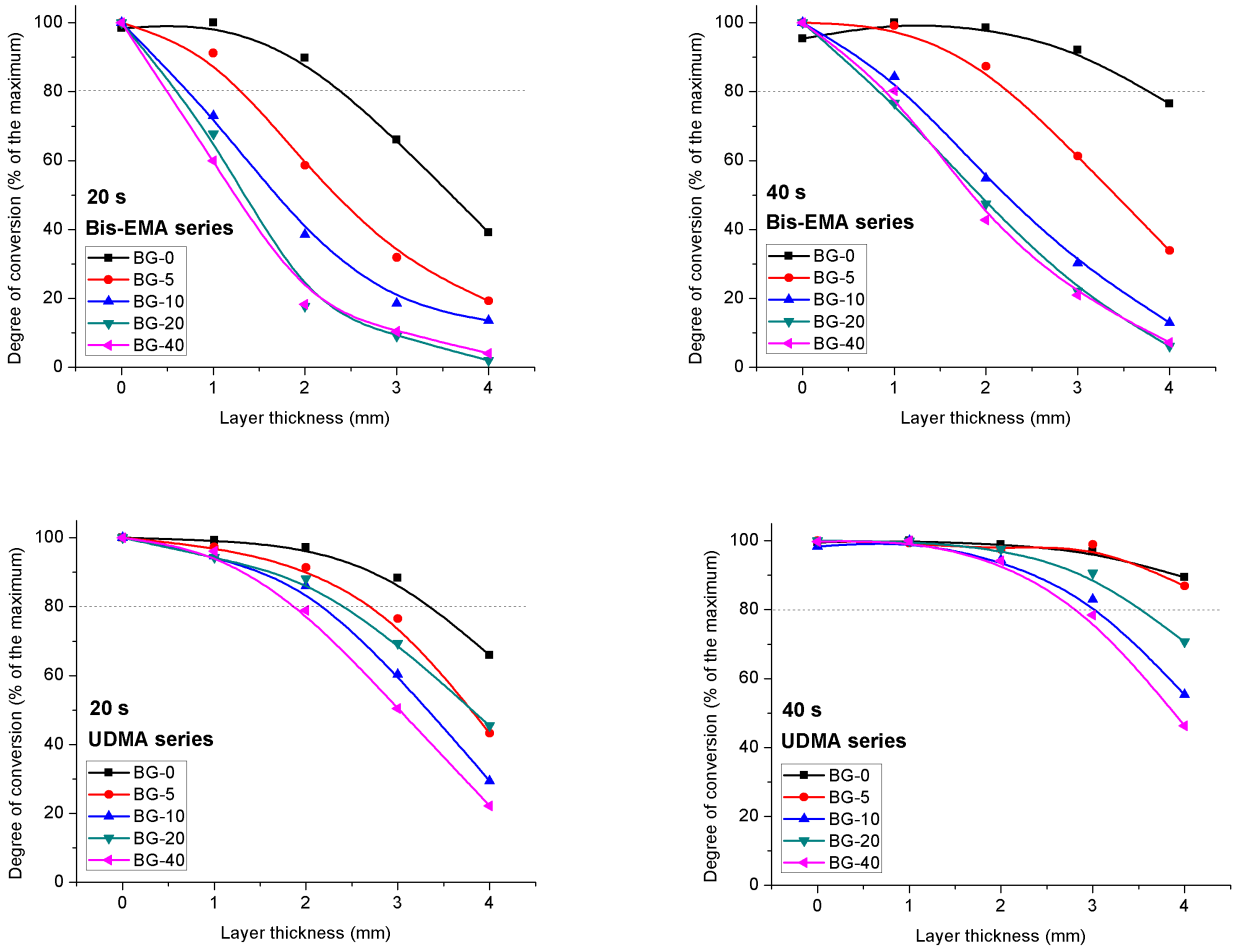

Figure 7. Curves of the degree of conversion as a function of layer thickness for experimental composites. The thickness at which the degree of conversion equals 80% of the maximum value (dotted lines) was considered as the depth of cure.

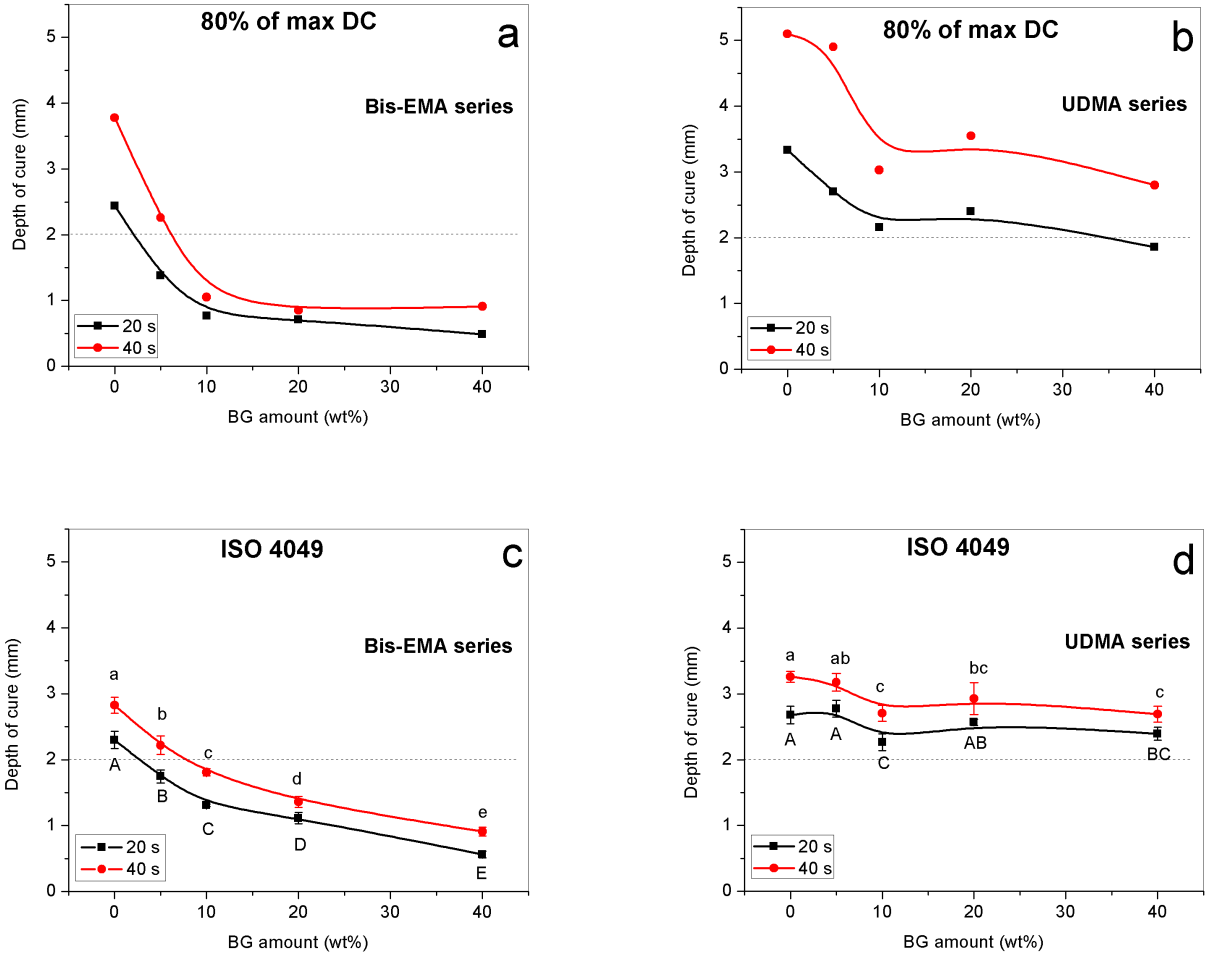

Figure 8. The depth of cure as a function of the BG amount, estimated as 80% of the maximum degree of conversion (a, b) and according to the ISO 4049 method (c, d). The dotted lines at 2 mm represent the “acceptable depth of cure” threshold. For the values obtained using the ISO 4049 method, same uppercase and lowercase letters denote statistically similar groups for curing time of 20 s and 40 s, respectively. Error bars indicate ± 1 s.d.

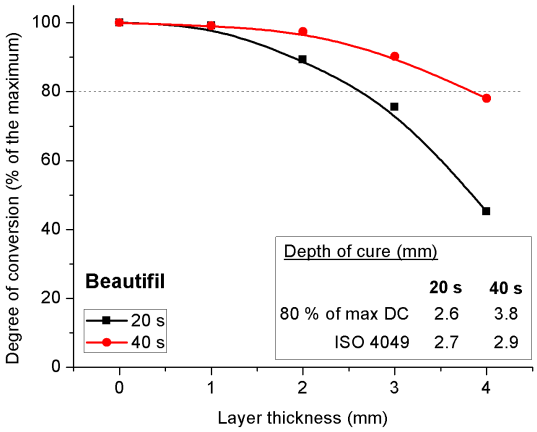

Figure 9. Curves of the degree of conversion as a function of layer thickness for the commercial reference material. The thickness at which the degree of conversion equals 80 % of the maximum value (dotted lines) was considered as the depth of cure. The inset shows the depth of cure values evaluated as 80% of the maximum degree of conversion and according to the ISO 4049 method.